RESEARCH ARTICLE

Rediscovery and redescription of *Niphargus enslini* Karaman, 1932 (Amphipoda, Niphargidae) in southern Germany

Dieter Weber[1], Traian Brad[2,3], Fabio Stoch[1], Jean-François Flot[1,4]

1 *Evolutionary Biology & Ecology, C.P. 160/12, Université libre de Bruxelles, Avenue F.D. Roosevelt 50, B-1050 Brussels, Belgium* **2** *Institutul de Speologie "Emil Racoviță", Str. Clinicilor nr. 5, 400006 Cluj-Napoca, Romania* **3** *Institutul Român de Știință și Tehnologie România Str. Virgil Fulicea nr. 3, 400022 Cluj-Napoca, Romania* **4** *Interuniversity Institute of Bioinformatics in Brussels – (IB)², Brussels, Belgium*

Corresponding author: Dieter Weber (dieter.weber124@gmx.de)

Citation: Weber D, Brad T, Stoch F, Flot J-F (2021) Rediscovery and redescription of *Niphargus enslini Karaman*, 1932 (Amphipoda, Niphargidae) in southern Germany. Subterranean Biology 40: 65–89. https://doi.org/10.3897/subtbiol.40.73017

Abstract

Niphargus enslini Karaman, 1932 was collected only once in 1905 from the Falkensteiner Höhle (Baden-Württemberg, Germany). Two years after its description, the species was synonymized with *Niphargus virei* and not studied any more. During recent surveys on German niphargids, further samples collected in this cave did not yield *N. enslini* specimens, but this species was collected in the Blätterteighöhle and in the Schwarzer Brunnen, two caves located in Baden-Württemberg and intercepting the same karstic aquifer feeding Falkensteiner Höhle. In an integrative taxonomic approach, we carefully studied the morphology of the newly collected specimens and sequenced two molecular markers (fragments of the cytochrome *c* oxidase subunit I (COI) and of the nuclear 28S rRNA gene) to test for possible conspecificity of *N. enslini* with *N. virei*. Morphological analysis confirmed that *N. enslini* is distinct from the *N. virei* species complex. We provide a redescription of newly collected material, together with new drawings of a more than 100 years old topotypic female. We briefly discuss the putative origin of *N. enslini* and the age of its split from the *N. virei* species complex.

Introduction

Species of the genus *Niphargus* Schiödte, 1849 have been intensively studied for more than 170 years and more than 400 species of this genus have been described so far (Horton et al. 2021). Seventeen species are reported from Germany (Spangenberg 1973; Dobat 1975, 1978; Weber 1991, 2012; Zaenker 2008), but the status of some of these were questioned (Schellenberg 1932, 1936; Weber et al. 2020a). Nearly all the descriptions of the German species were performed using morphological characters alone.

Niphargus enslini Karaman, 1932 was described based on four specimens collected in 1905 in the Falkensteiner Höhle by Eduard Enslin. Karaman's (1932) description and drawings corresponded to the taxonomic standards of their time but are nowadays considered poor and incomplete. Karaman (1932) suggested that *N. enslini* was closely related in morphology and habitus to *Niphargus orcinus* Joseph, 1869 (a Slovenian species, at that time confused with the French *Niphargus virei* Chevreux, 1896). A holotype was not defined, so all the four specimens used in original description must be considered as syntypes.

One year later, Schellenberg (1933a) stated that he considered *N. enslini* as a subspecies of *N. orcinus*, and later (Schellenberg 1933b) synonymized it with *N. virei* (as *N. orcinus virei*). Although in the WoRMS database (Horton et al. 2021) *N. enslini* is still reported as an independent species, there was no justification supporting this statement up to now. In fact, *N. enslini* was never re-collected in the Falkensteiner Höhle, neither by Boris Sket before 1966 (Dobat 1975), nor by Günzler (1964) and Dobat (1975), who found in the cave only the widespread *Niphargus puteanus* (Koch, 1936). For this reason, no further material existed apart the type series to accept or reject Schellenberg's (1933a, b) hypothesis. Unfortunately, Karaman's material is not available for study and his collection is inaccessible, being no more present in the Montenegrin academy of Sciences and Arts, Podgorica, Montenegro (Vladimir Pešić, personal communication).

After a collecting gap of 112 years, we found again specimens that could be ascribed based on their morphology to *N. enslini* in two caves in the Swabian Alb, Southern Germany. This discovery gave us the opportunity to test Schellenberg's (1933b) synonymy. The aims of the present article were therefore (i) to use molecular taxonomy to characterize *N. enslini* and allocate it within the phylogenetic tree of niphargid amphipods; (ii) to use molecular species delimitation methods to test the specific status of *N. enslini*, and (iii) to redescribe it accurately, following modern morphotaxonomical standards, highlighting its morphological peculiarities.

Material and methods

Sampling

From 2016 to 2019, one of the authors (D.W.) collected 1,705 niphargid specimens from 85 springs, 13 natural caves, two artificial cavities, and two interstitial sites in

Baden-Württemberg, Germany. Most specimens were collected by opportunistic sampling, putting mud and organic material onto sieves with a mesh size of 5 to 0.2 mm and washing with water to find and collect specimens. In few cases, niphargids were collected by eye using spring steel forceps or by means of baited traps.

Our sampling survey in Baden-Württemberg included Falkensteiner Höhle, the type locality of *Niphargus enslini* located between the city of Bad Urach and the village of Grabenstetten (both in the administrative district of Reutlingen, southern Germany). It is an active limestone cave more than 4,000 m long. Using three baited traps placed in the water basins in the first 400 m of the cave, we collected 77 specimens of *Niphargus puteanus* (Weber et al. 2020a), but no *N. enslini*. In Elsachbröller, a karstic cave close to the Falkensteiner Höhle and in several springs close by, we also found *N. puteanus*, but never *N. enslini*.

Four specimens morphologically attributable to *Niphargus enslini* were found on 26–27 August 2017 in the Blätterteighöhle (cave inventory number 8119/29; WGS 84 coordinates: 47.8463°N, 8.8589°E; altitude 478 m a.s.l., city of Aach, administrative district of Konstanz, Baden-Württemberg, southern Germany: Grimm 2020). The Blätterteighöhle (Fig. 1A) is a 138 m long (Grimm 2015), natural cave in limestone, very close to the Aachquelle, which is the karstic spring with the highest discharge in Germany (http://www.aachquelle.de/). The cave, accidentally discovered in 2005, is locked and administrated by the Freunde der Aachhöhle (http://www.aachhoehle.de/). The specimens were collected in 2017 from a small pool 10 m inside the cave using liver baited traps. Several trials performed at the end of 2019 to recollect specimens failed.

Another *N. enslini* specimen was found on 5 August 2017 in the Schwarzer Brunnen (literally 'Black Well'; cave inventory number 7720/62, WGS 84 coordinates: 48.2746°N, 9.0606°E; altitude 799 m a.s.l.). The Schwarzer Brunnen (Fig. 1B) is a nearly 1,000 m long cave in limestone, in the communal district of the city of Burladingen (Zollernalbkreis, Baden-Württemberg, southern Germany). It is close to the border separating the Rhine River and Danube River basins (Schetter et al. 2017), discharging into the Neckar river and close to a 30 km long graben (the Hohenzollerngraben) striking in the Hercynian direction. Niphargids were collected in the Schwarzer Brunnen before 2017 but never properly described (Schetter et al. 2017). However, our attempt to re-collect there on 14 August 2019 failed.

In the Wimsener Höhle (Hayingen-Wimsen, Swabian Alb, Baden-Württemberg, Germany), Straub (2013) reported *Niphargus virei* (collected 24 February 2007, Rainer Straub, personal communication). The presence of *N. virei* far to the east of its distribution area and not far away from the sites where *N. enslini* had been found seemed quite improbable. The specimen on which the determination was based has been lost, and, unfortunately, an attempt to re-collect niphargids on 17 August 2019 failed.

Finally, the Umweltgruppe Kirchheim (http://www.uwg-kirchheim.de/HTML/N2/tiereundpflanzen2_3.html, accessed 7th April 2020) mentioned *N. enslini* from the Buchbrunnenquelle close to Dischingen (WGS84 coordinates: 48.695°N, 10.363°E), based on a report from the Fachhochschule Magdeburg. The Hochschule Magdeburg-Stendal (Uta Langheinrich, email dated 17 April 2020) communicated that *N. enslini*
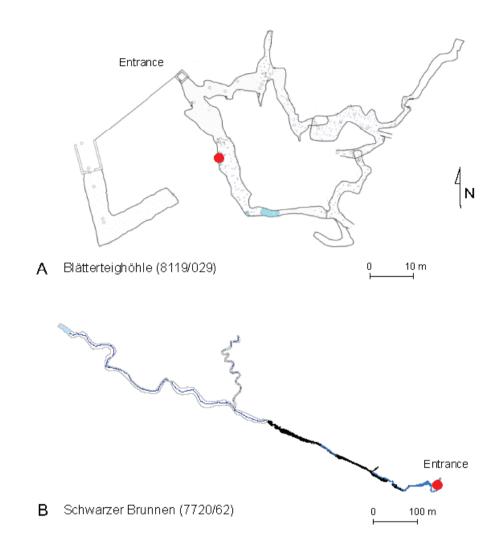
Figure 1. Plan of the two sampled caves. Sampling sites are marked with a red dot. Map kindly provided by Freunde der Aachhöhle (Blätterteighöhle) and Raphael Grimm (Schwarzer Brunnen), modified.

was never found by the Fachhochschule Magdeburg or the Hochschule Magdeburg-Stendal. The report from the Buchbrunnenquelle is thus not confirmed.

The locations of the sampling sites of *N. enslini* are reported in Fig. 2; sites are superimposed on the map of the aquifers of this sector of Baden-Württemberg.

Museum material examined

One female specimen from the Falkensteiner Höhle stored in the crustacean collection of the Natural History Museum of Berlin, collection GBIF Crustacea – ZMB Berlin,
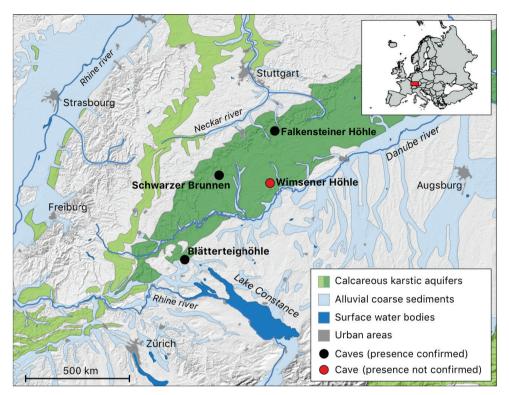
Figure 2. Distribution of *Niphargus enslini*. Black circles indicate the type locality and the new sampling sites; Wimsener Höhle where *Niphargus virei* is cited is reported in red. All the sites are clearly located in the same karstic aquifer. The record from Buchbrunnenquelle is not indicated here as it is probably erroneous.

No. 24795, leg. Enslin, determined by Schellenberg as *Niphargus orcinus virei*. This specimen, a badly preserved female, is probably one of those described as *Niphargus enslini* by Karaman (1932) from the same cave (leg. Enslin, July 1905, 4 specimens, 1 male and 4 females), and it is the specimen studied by Schellenberg (1933a).

Molecular analyses

One pereopod, removed from each of four specimens of *Niphargus enslini*, was used for DNA extraction, and the remaining body parts and appendages of each specimen were stored in 96% ethanol at -20 °C at the Université libre de Bruxelles (ULB), Belgium. Genomic DNA was extracted using the NucleoSpin@ Tissue kit by Macherey-Nagel, following the manufacturer's protocol. The eluted DNA was stored at 4 °C until amplification then long-term stored at -20 °C.

A fragment of the nuclear 28S rRNA gene and a 658 bp fragment of the mitochondrial cytochrome *c* oxidase subunit I (COI) were amplified using the primers described by Verovnik et al. (2005) for 28S and by Astrin and Stüben (2008) for COI. A list of the primers and PCR amplification protocols used is reported in Suppl. material 1: Table S1.

Direct sequencing was performed using the same primers as for amplification and/or using internal primers (see Flot et al. 2010; Weber et al. 2020b; Suppl. material 1: Table S1); PCR products were sent for bidirectional Sanger sequencing to Genoscreen (Lille, France).

Chromatogram inspection and sequence editing were performed in Sequencher version 4.1.4 (Gene Codes). No double peaks suggesting 28S heterozygotes were observed in this set of chromatograms.

To assess the position of the *N. enslini* species complex within the phylogenetic tree of Niphargidae, 232 Niphargidae species were used together with four species of the family Pseudoniphargidae (genera *Pseudoniphargus* and *Microniphargus*) as outgroups, since the latter was suggested to be the sister group of Niphargidae in recent studies (Jurado-Rivera et al. 2017; Weber et al. 2020b). For this phylogenetic analysis, we assembled a molecular dataset including 233 sequences of a 28S rRNA gene fragment downloaded from GenBank, supplemented by three new sequences, two of *N. enslini* and one of *Carinurella paradoxa*, obtained using the techniques described above (morphospecies names and GenBank accession codes of the 236 sequences used in the analysis are listed in the Suppl. material 1: Table S2).

28S sequences were aligned using the E-INS-i algorithm implemented in MAFFT 7 (Katoh et al. 2019). Phylogenetic relationships were reconstructed using maximum likelihood and 1,000 ultrafast bootstrap replicates in IQ-TREE2 (Minh et al. 2020), using the optimal substitution model (GRT+F+R4, coded following the IQtree2 manual) selected using ModelFinder (Kalyaanamoorthy et al. 2017) according to the Bayesian Information Criterion (Schwarz 1978).

COI sequences (Suppl. material 1: Table S3), including four sequences of the *Niphargus virei* species complex downloaded from Genbank, three sequences of *N. enslini* and five new sequences of the *N. virei* species complex (according to Léfebure et al. 2006 named *N. virei* species A, B, C) obtained using the methods reported above, were used to produce a median-joining haplotype network using the HaplowebMaker web server (https://eeg-ebe.github.io/HaplowebMaker/; Spöri and Flot 2020). Putative species were inferred using COI by applying the Automatic Barcode Gap Analysis (ABGD) method (Puillandre et al. 2012: https://bioinfo.mnhn.fr/abi/public/abgd/abgdweb.html) on the resulting alignment. The Jukes-Cantor (JC69) distance was selected, and ABGD was run on the public webserver with default parameters, except for the number of steps which was set to 100 to achieve more stable results.

All chromatograms and FASTA alignments were uploaded to Zenodo (Weber et al. 2021).

Morphological analyses

One sexually mature male and one female with well developed oostegites from the Blätterteighöhle as well as the adult female from the Falkensteiner Höhle preserved in the Berlin Museum were dissected in glycerol; their appendages were mounted in Kaiser's glycerol gelatine (Merck, Germany) and inspected with an Olympus SZX16
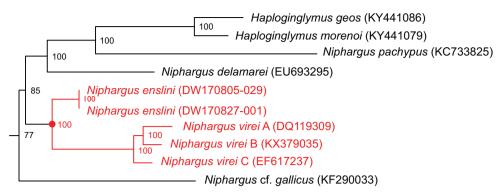
Figure 3. A subset of the phylogenetic tree with *Niphargus enslini* and its closest neighbours of the *Niphargus virei* sister group, reconstructed using maximum likelihood (IQTree2), based on a fragment of the 28S rRNA gene. Ultrafast bootstrap supports are shown on nodes. The *N. virei* clade, which includes *N. enslini* (100% support), is reported in red. A full tree is shown in the Suppl. material 1: Fig. S1.

stereomicroscope and an Olympus BX51 microscope. Drawings were performed either manually by reproducing on transparent paper the photographs taken with the microscope camera or using a camera lucida and digitally inking the pencil drawings using Adobe Illustrator drawing software. Systematic microscope inspection of the slides with specimens' appendages ensured the addition of finer details that could not be seen on photographs or preliminary drawings due to the thickness of mouthparts and appendages.

Results

Molecular analyses

The phylogenetic analyses based on 28S rDNA using 232 Niphargidae species (and representatives of the family Pseudoniphargidae as an outgroup), reported in Suppl. material 1: Fig. S1, pointed to *Niphargus enslini* as the sister clade of the *Niphargus virei* species complex. Bootstrap support (100%) confirmed the monophyly of the *N. enslini* + *N. virei* species complex, as well as the monophyly of the *N. virei* species complex. A detail of the 28S ML tree is reported in Fig. 3 to clarify the relationships within this clade (*N. virei* A, B, and C are the acronyms used by Léfebure et al. 2006 in their attempt to separate three putative cryptic species within the *N. virei* species complex).

The haplotype network based on COI (Fig. 4) clearly confirmed the separation of the four species within the target clade, showing that *N. enslini* is the species with the greatest genetic distance from other ones. ABGD applied to this dataset returned four distinct primary species hypotheses, confirming the results obtained by the visual examination of the network.
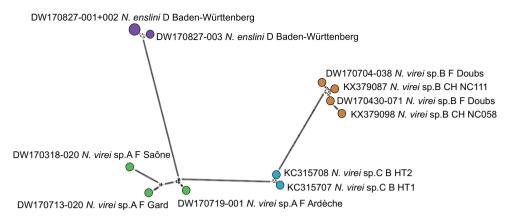
Figure 4. Haplotype network of COI of the *Niphargus enslini – Niphargus virei* clade (original data and data downloaded from GenBank). Colors distinguish the four putative species delimited by applying ABGD to the COI *Niphargus* dataset.

Morphological redescription

Order Amphipoda Latreille, 1816
Family Niphargidae Bousfield, 1977
Genus *Niphargus* Schiödte, 1849

***Niphargus enslini* Karaman, 1932**
Figures 6–13

syn: *Niphargus orcinus enslini* Schellenberg (1933a); *Niphargus orcinus virei* (Schellenberg, 1933b)

Material examined. Male. Germany, 1 ♂; Blätterteighöhle; 26–27 August 2017; Bernd Hugger, Rafael Grimm, Dieter Weber leg. The specimen was dissected and used for species redescription. The dissected body appendages were transferred to permanent slides and stored in the collection of the Université libre de Bruxelles (ULB) under voucher number: 170827-004.

Females. Germany, 3 ♀♀; Blätterteighöhle; 26–27 August 2017; Bernd Hugger, Rafael Grimm, Dieter Weber leg. One female (Voucher number: 170827-001) was dissected and used to study the sexual dimorphism. Two females were not dissected and are preserved in 96% ethanol at -20 °C in the collection of the Université libre de Bruxelles (ULB), Belgium. Voucher numbers: 170827-002 and 170827-003. Germany, 1 ♀, Falkensteiner Höhle, leg. Enslin, partially dissected and mounted on a slide stored in the crustacean collection of the Natural History Museum of Berlin (GBIF Crustacea – ZMB Berlin, No. 24795).

Juveniles. Germany, 1 juv. (voucher number 170805-029); Schwarzer Brunnen; 5 August 2017; Harald Knupfer leg. The specimen was far too small for morphological determination and was completely used for DNA extraction.

Figure 5. *Niphargus enslini*, live male from the Blätterteighöhle (Photo: Bernd Hugger).

All DNA isolates are stored at −20 °C at the Université libre de Bruxelles (ULB) in the research unit Evolutionary Biology & Ecology. Voucher numbers: 170827-001, 170827-002, 170827-003, 170805-029.
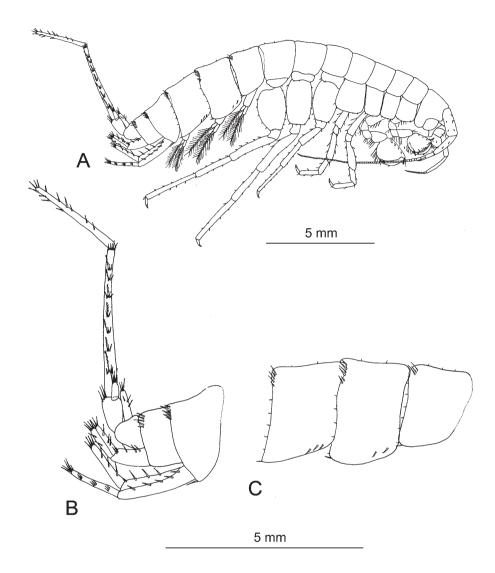
Diagnosis. Robust, mid-sized *Niphargus*. Right to acute postero-ventral angle of epimeral plates. Pleon with 3–6 spines on the postero-dorsal side of each segment. Gnathopods coxae trapezoidal with only one thin seta along the outer margin of dactylus. Coxal plate IV sub-rectangular, with no posterior protrusion. Pereopod VI reaching more than half of the total body length. Uropod I rami subequal. Uropod III sexually dimorphic; exopod elongated in males. Telson relatively elongated in males, bearing 4 apical, 4–5 lateral and 3–5 smaller dorsal spines on each lobe.

Description of male. Habitus as in Fig. 5. Body length (measured from anterior part of head to telson insertion) of the single male examined 19.6 mm (Fig. 6). All detailed measurements on body appendages were performed according to the methods described in Fišer et al. (2009) and are reported in Suppl. material 1: Table S4.

Head (Fig. 6A) without rostrum representing 7.2% of total body length.

Antenna I (Fig. 7A), longer than half of total body length (Suppl. material 1: Table S2), with main flagellum formed of 48 articles. All articles in the distal two thirds of flagellum bear one aestethasc (Fig. 7D) as long as one half of the respective article. Length of antenna I peduncle almost one third of total length of antenna I. Accessory flagellum formed of 2 articles (Figs 7B, C); proximal article length slightly exceeding the first article of main flagellum; distal article bearing 2 apical setae and 1 aestethasc and represents slightly less than one third of the total length of the accessory flagellum.

Antenna II (Fig. 7E) with flagellum formed of 18 articles, almost half of total length of antenna I. Antennary peduncle almost twice as long as flagellum.

Figures 6. *Niphargus enslini*, male from the Blätterteighöhle **A** habitus **B** urosomites and uropods **C** epimeral plates.

Labrum of typical, subovoid shape.

Lower lip (Fig. 8A) with inner lobes slightly shorter than outer lobes. Inner lobes with thin distal setae. Outer lobes with two rows of thin setae subapically on both sides.

Left mandible (Fig. 8B) with 3 teeth on incisor process and 4 teeth on lacinia mobilis. Ten serrated setae alternated with sensory setae between lacinia mobilis and molar process (pars molaris).
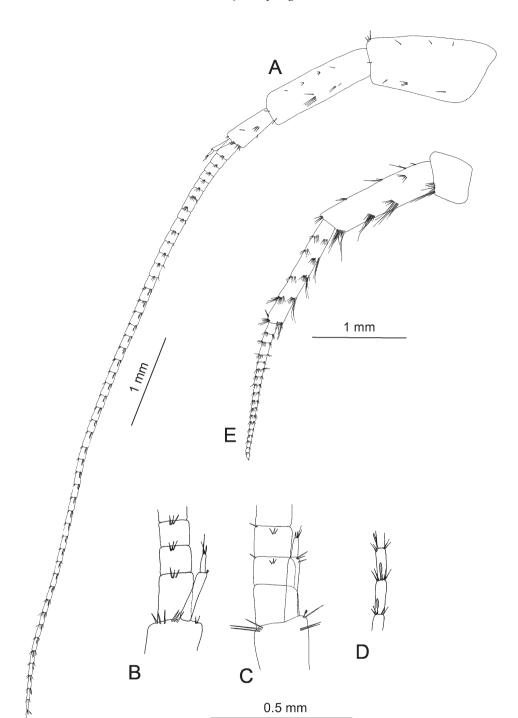
Figure 7. *Niphargus enslini*, male from the Blätterteighöhle **A** antenna I **B, C** accessory flagellum of antenna I **D** aesthetascs on antennulary segments of flagellum **E** antenna II.
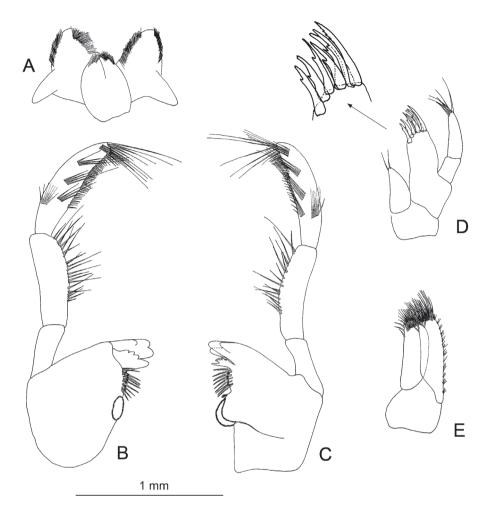
Figure 8. *Niphargus enslini*, male from the Blätterteighöhle **A** labium **B** left mandible **C** right mandible **D** maxilla I **E** maxila II.

Right mandible (Fig. 8C) with 4 teeth on incisor process, several small denticles on lacinia mobilis; a row of 9 serrated setae and 5 sensory setae between lacinia mobilis and molar process; a long seta proximal to molar process.

Mandibulary palps (Figs 8B, C) of both sides subequal. The three articles of mandibulary palp account for 19.8% (article 1), 37.1% (article 2) and 43.1% (article 3) of the total length of the palp (Suppl. material 1: Table S2). Proximal article without setae, article 2 with 18–22 ventral setae and distal article of the palp with one group of 8 A-setae on the outer face, 4 groups of B-setae on the inner face with 4 setae each, 28–34 D-setae and 7–9 E-setae.

Maxilla I (Fig. 8D) with 6 apical setae on the distal article of the palp. Outer lobe with 6 spines with one tooth each and one spine with several smaller teeth. Inner lobe with 2 apical setae.
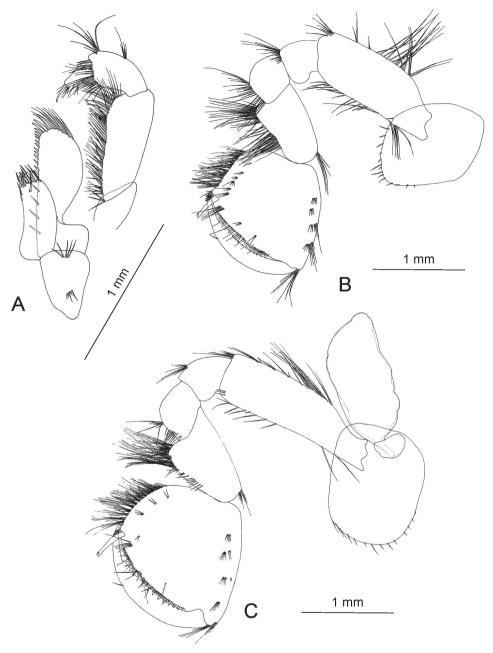
Figure 9. *Niphargus enslini*, male from the Blätterteighöhle **A** maxilliped **B** gnathopod I **C** gnathopod II.

Maxilla II (Fig. 8E) with inner lobe slightly shorter than outer lobe. Each lobe bearing 2 rows of setae, one apical and one subapical. A row of thin setae along the outer margin of outer lobe.

Maxilliped (Fig. 9A) with palp formed of four articles. Article 1 without setae, article 2 with numerous setae aligned along the inner margin. Article 3 with one group of

12 setae located on the inner margin, one group of 11 apical setae, of which 5 serrated, and two groups of 4 and 7 setae on the outer margin. Article 4 with a row of 6 setae on the inner margin and one seta located on the outer margin. Outer lobe of maxilliped with 5 shorter setae, 14 flattened spiniform setae and 8 longer setae located apically. Inner lobe provided apically with 5 flattened spines, 6 serrated and 4 normal setae.

Gnathopod I (Fig. 9B) with a rhomboidal coxal plate larger than wide (ratio depth:width 1.0:0.7). Basipod length:carpus length 1.0:0.5. Ischium with one posteroventral group of 15 setae. Carpus with a row of 45 setae of various lengths along ventral margin, and one group of 5 setae located anterodorsally. Propodite approximately as long as wide and with several groups of 4–6 setae on its ventral margin, one antero-dorsal group of 9 setae and one antero-apical group of 9 setae. Six facial groups with 1–4 setae each on outer surface of propodite close to its ventral side and three groups of 4–7 setae close to the dorsal margin. One group of 6 long setae near palmar corner. Strong palmar spine and 2 supporting spines at palmar corner. Dactylus with nail length almost one third of total dactylus length and with one small seta along outer margin.

Gnathopod II (Fig. 9C) larger than gnathopod I with a rectangular coxal plate (ratio depth:width 1.0:0.8). Ovoid gill, with a length equal to that of the coxal plate. Basis length:width ratio 1.0:0.3. Ischium with one posteroventral group of 6 setae. Basis length:carpus length ratio 1.0:0.5. Carpus with 8 groups of 4–6 setae along its ventral margin, a row of 15 setae on its surface close to ventral margin and a group of 7 setae located anterodorsally. The propodite approximately as long as wide, with several groups of 4–6 setae on its ventral margin, one antero-dorsal group of 5 setae and one antero-apical group of 9 setae. On its outer surface, propodite with 4 groups of 2–3 setae located close to its ventral margin, 3 groups formed of 5–8 setae closer to the dorsal margin, one group of 4 long setae close to the palmar spine and one seta located medially on the anterior side of the propodus. Strong palmar spine and two supporting spines at palmar corner. Dactylus with nail length one third of total dactylus length and with one small seta along outer margin.

Pereopod III (Fig. 10A) with rectangular coxal plate, ratio depth:width 1.0:0.7. Gill of similar shape and size. Propodite length:dactylus length ratio 1.0:0.5. Dactylus with nail measuring almost half of total length of dactylus, with one dorsal seta with plumose tip and one spine and one tiny seta at nail base. Pereopod III nearly equal in length to pereopod IV (pereopod III length:pereopod IV length ratio 1.0:0.91).

Pereopod IV (Fig. 10B) with coxal plate sub-rectangular, with a concavity on the posterior margin. Depth:maximum width ratio 1.0:1.0. Robust dactylus, with nail measuring almost half of total dactylus length; with one dorsal seta with plumose tip and one spine accompanied by a tiny seta near nail base. Propodite length:dactylus length ratio 1.0:0.5.

Pereopod V (Fig. 10C) with coxal plate of irregular shape, with a deep concavity on the ventral side and two anterior setae. Gill ovoid to trapezoidal. Basis ovoid-rectangular with length:width ratio 1.0:0.7 with 20 short and thick setae on posterior
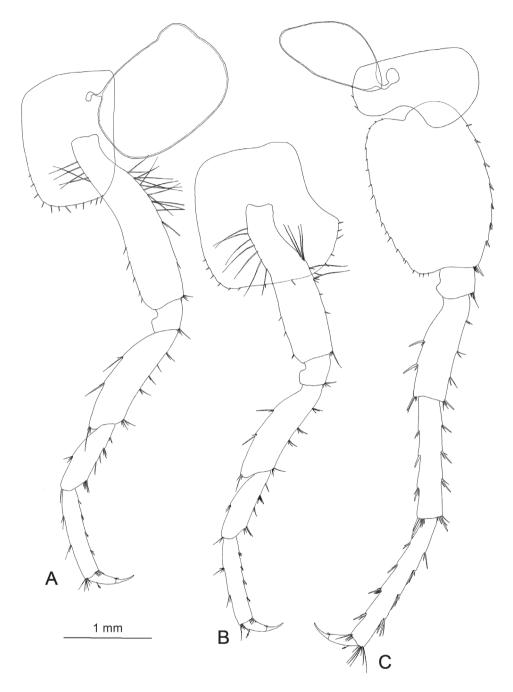
Figure 10. *Niphargus enslini*, male from the Blätterteighöhle **A** pereopod III **B** pereopod IV **C** pereopod V (dactlylus twisted).

margin, and 7 groups of 1–3 similar setae on anterior margin. Dactylus with one plumose seta on outer margin and one spine and one seta at nail base, which represents 40% of the total dactylus length. Propodite length:dactylus length ratio 1.0:0.3.

Pereopod VI (Fig. 11A) more than 11 mm long, being the longest leg of the inspected male. Coxal plate less robust compared to that of pereopod V, but highly similar in shape, with three posterior setae and two ventral setae. Basipodite with ovoid-trapezoidal shape, 11 small setae on posterior margin and six groups of 1–2 setae on anterior margin; length:width ratio 1.0:0.65. Dactylus with one plumose seta on outer margin and one spine and a tiny seta near nail base. Nail length slightly more than one third of the total dactylus length. Ratio propodite length:dactylus length 1.0:0.3.

Pereopod VII (Fig. 11B). Coxal plate trapezoidal, with three setae on the posterior margin. Basis ovoid-trapezoidal, with a ratio length:width 1.0:0.7. Basis bearing 19 setae on posterior margin and five groups of 2–3 thick setae on anterior margin. Dactylus with one seta on the outer margin and one seta accompanied by one spine near nail base. Nail length one third of total dactylus length. Ratio propodite length:dactylus length 1.0:0.3.

Pereopods V:VI:VII ratio 1.0:1.32:1.27.

Pleopods similar each other (pleopod I as in Fig. 11C), with unequal rami and two retinacles on peduncle.

Uropod I (Fig. 12A) with two dorso-lateral rows of 4 spines on peduncle. Endopodite and exopodite of same length. Exopodite more setose than endopodite. One strong spine near the insertion of uropod I.

Uropod II (Fig. 12B) with four dorsolateral spines on peduncle. Endopod longer than exopod, endopod length:exopod length ratio 1.0:0.82, both rami with a low number of spines.

Uropod III (Fig. 12C) 8.6 mm long, which makes it almost as long as half of total body length. Peduncle with two groups of 4 apical spiniform setae each. Endopod short, about half the length of peduncle, with 4 simple setae and one plumose seta apically. Proximal segment of exopod longer than distal segment (ratio 1.0:0.6). Outer margin of the proximal segment of exopod with 7 groups of setae, almost every group containing one plumose seta; inner margin with 4 groups of 5 small setae each. Distal segment of exopod provided with two groups of 4 setae in its second half and one subapical group of 5 setae on the anterior margin, one subapical row of 4 small setae on the posterior side and several setae of different lengths located apically.

Epimeral plates (Fig. 6C). Epimeral plate I with acute to right postero-ventral angle, relatively straight ventral margin with no spines and concave posterior margin with 7 setae and three postero-dorsal setae. Epimeral plate II with right postero-ventral angle, convex ventral margin with two spines and relatively straight posterior margin with 6 setae and 6 postero-dorsal setae. Epimeral plate III is slightly different compared to epimeral plates I and II, the postero-ventral angle is rather acute, the ventral margin is relatively straight with 3 spiniform setae, the posterior margin is concave to straight, with 6 setae and 5 postero-dorsal setae.
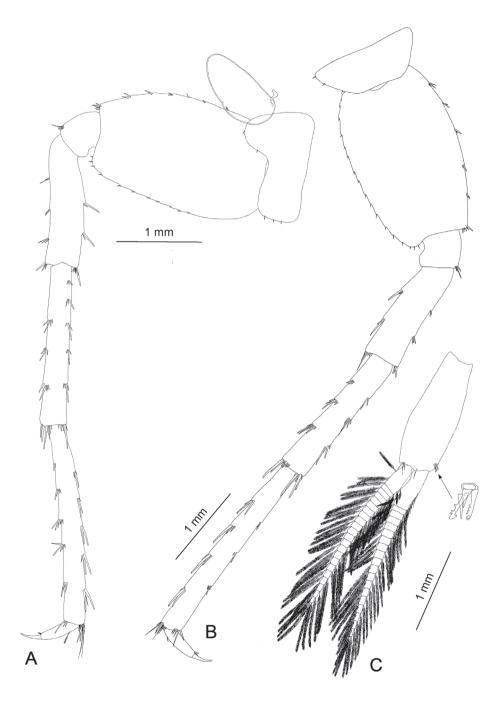
Figure 11. *Niphargus enslini*, male from the Blätterteighöhle **A** pereopod VI **B** Pereopod VII **C** pleopod I (enlarged: retinacula).
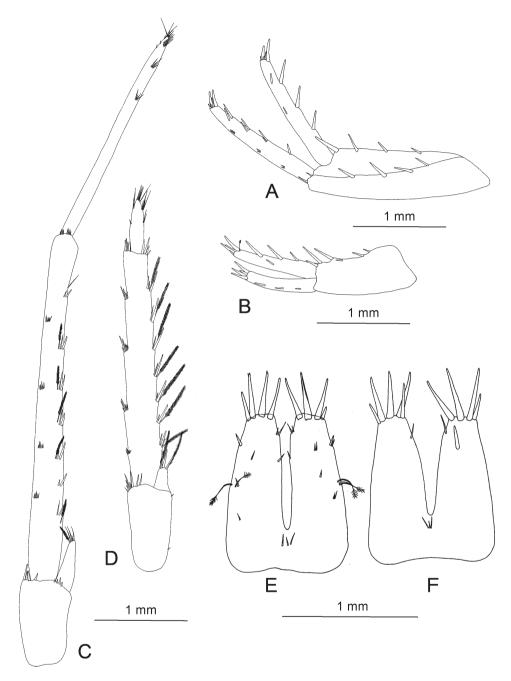
Figure 12. *Niphargus enslini*, male from the Blätterteighöhle **A** uropod I **B** uropod II **C** uropod III **E** telson. Female from the Blätterteighöhle: **D** uropod III **F** telson.
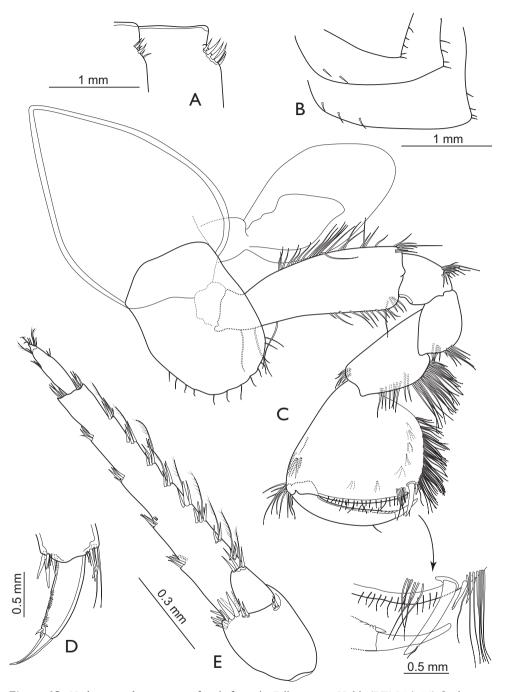
Figure 13. *Niphargus enslini*, topotype female from the Falkensteiner Höhle (BZM 24795) **A** pleonites 2–3, dorsal margin with spines **B** epimeral plates 1–3 (left side) **C** gnathopod II with gill and oostegite (enlarged: the palmar corner), outer side **D** dactylopodite of pereopod 7 **E** uropod III (left).

Urosomite I (Fig. 6B) with 7 dorso-lateral setae on each side of posterior margin, urosomite II with 5 dorso-lateral setae of various lengths on each side of posterior margin. Posterior margin of urosomite III without setation.

Telson (Fig. 12E) longer than wide (length:width ratio 1.0:0.75), with 4 apical spines of different lengths. Longest spine slightly shorter than one third of telson length. Two thin setae with plumose tips along each side. 4–5 lateral and 3–5 dorsal spines on each lobe.

Sexual dimorphism. Male and female highly similar except for the presence of oostegites (Fig. 13C), uropod III and telson. Uropod III of female (Figs 12D, 13E) shorter compared to that of male; second article of exopod shorter than in male, slightly longer than endopod. Female telson (Fig. 12F) similar in shape and size to that of male, but with lower number of spines laterally and dorsally. Female telson missing the lateral plumose setae.

Comparison between the female from the Falkensteiner Höhle (type locality) and the female from the Blätterteighöhle could not detect marked differences. The small differences that could be noticed observing Karaman's (1932) drawings disappeared after a careful examination of the dissected appendages (Fig. 13), confirming that they were due to the poor quality of the original description. The shape of the propodite of the second gnathopod (Fig. 13C) is very similar, and the presence of minute groups of spinules on its outer surface, not reported in Karaman's (1932) figure 6, was confirmed in the specimen examined (Fig. 13C). Only a minor difference was observed in the length of the apical spines of the endopod of uropod III (Fig. 13E), which are slighter shorter in the female from the type locality in comparison to the one of the Blätterteighöhle. However, the very low number of specimens examined did not allow us to ascertain the variability of this character in different populations of the species.

Discussion

Niphargus enslini is a distinct species from the *Niphargus virei* species complex; the distinction is supported both by molecular and morphotaxonomical data. The 28S phylogenetic tree clearly shows that *N. enslini* is the sister taxon of the *N. virei* species complex. COI haplotype network analyses and ABGD species delimitation method confirmed that the known populations of this clade can be ascribed to four putative species, i.e., *N. enslini* and *N. virei* A, B, and C (Léfebure et al. 2006). Morphological analysis clearly shows that *N. enslini* can be easily distinguished from the *N. virei* species complex. The shape of the coxal plate IV, posteriorly produced, which is so characteristic of the *N. virei* species complex as to be used as the main distinguishing character of the species (together with the very small *Niphargus laisi* Schellenberg, 1936) from all other niphargids in the identification key by Ginet (1996), is different in *N. enslini*, lacking the posterior protrusion. The slender telson and the subequal rami of uropod I in the adult male are further discriminating characters between *N. enslini* and the *N. virei* species complex.

Around the Blätterteighöhle, Bernasconi (1994) and Fuchs (2007) assessed the presence (on a morphological basis) of the following small-sized species: *Microniphargus leruthi* Schellenberg, 1934; *Niphargus auerbachi* Schellenberg, 1934; *Niphargus kieferi* Schellenberg, 1936; and *Niphargus laisi* Schellenberg, 1936. These species were found mainly in interstitial environments. Using molecular techniques, we identified around the Blätterteighöhle a new species of the *Niphargus aquilex* Schiödte, 1855 species complex (Weber, unpublished) but mainly *Niphargus puteanus* Koch, 1836 (Weber et al. 2020a). *N. puteanus* was found in the Donauhöhle located 500 m North of the Blätterteighöhle. Despite intensive sampling, no other sites for *N. enslini* were discovered, leading us to believe that this is a rare species.

Interestingly, all three caves where *N. enslini* was reported discharge in different river watersheds (the Neckar River and the Rhine River – flowing to the North Sea – and the Danube River – flowing into the Black Sea: Fig. 5). However, *N. enslini* was found in a single large karstic aquifer, and it is well known that aquifers do not correspond to the epigean watersheds where their water is drained. For this reason, significant differences in groundwater biodiversity can be detected between aquifers, whereas differences among hydrogeographic basins may be negligible (Galassi et al. 2009).

Moreover, *N. enslini* was only found in sites that were not covered by glaciers during the Last Glacial Maximum (Glückert 1987) but are located very close to the border of Quaternary glaciers. A similar distribution was already observed for the *N. virei* species complex (Foulquier et al. 2008) with its main distribution area located west of the Alps and nearly never overlapping with formerly glaciated areas. However, the distribution areas of *N. enslini* and the *N. virei* species complex are not separated by the Alpine chain, but by the Swiss Jura. It can be assumed that the common ancestor of these species was widely distributed across Southern France, Switzerland, and Southern Germany.

Two biogeographic scenarios can be proposed to explain the isolation of the whole species group into two clades (i.e., *N. enslini* and the *N. virei* species complex).

In the first scenario, the orogenesis of the Jura massif in late Tortonian and early Messinian (around 6.6–8.6 Ma: Becker 2000) split the distribution area of the common ancestor and allopatric speciation begun. During Quaternary glaciations (started 1.9 Ma), the two species enlarged their distribution areas, which never overlapped due to mountain barriers.

In the second scenario, the most recent common ancestor of the *N. virei* species complex and of *N. enslini* could have transgressed the Jura watershed, and the split should have occurred later during Quaternary glaciations.

Previous attempts to date the split of the *N. virei* species complex clade from the other niphargids, based on different molecular clocks, support the hypothesis of a rather old event: McInerney et al. (2013) suggested around 23 Ma, Delić et al. (2019) found a value of 15 (6.5–19) Ma, whereas the most recent multimarker chronogram built by Borko et al. (2021) suggested a lower value of 7.5 (5–11) Ma. Despite their high degree of uncertainty, these datings tend to reject the second scenario and we assume that the split between *N. enslini* and the *N. virei* species complex started around 6.6–8.6 Ma, as suggested by the paleogeographical evidence.

Acknowledgements

References

Astrin JJ, Stüben PE (2008) Phylogeny in cryptic weevils: molecules, morphology and new genera of western Palaearctic Cryptorhynchinae (Coleoptera:Curculionidae). Invertebrate Systematics 22: 503–522. https://doi.org/10.1071/IS07057

Becker A (2000) Der Faltenjura: geologischer Rahmen, Bau und Entwicklung seit dem Miozän. Jahresberichte und Mitteilungen des Oberrheinischen Geologischen Vereins 82: 317–336. https://doi.org/10.1127/jmogv/82/2000/317

Bernasconi R (1994) Suisse (Schweiz/Svizzera). Encyclopaedia Biospeologica 1: 809–818.

Borko Š, Trontelj P, Seehausen O, Moškrič A, Fišer C (2021) A subterranean adaptive radiation of amphipods in Europe. Nature Communications 12: e3688. https://doi.org/10.1038/s41467-021-24023-w

Chevreux E (1896) Sur un Amphipode d'eau douce, *Niphargus Virei* nov. sp., provenant des grottes du Jura. Bulletin du Muséum d'Histoire Naturelle 2: 136–137.

Delić T, Stoch F, Borko Š, Flot J-F, Fišer C (2020) How subterranean amphipods crossed the Adriatic Sea? Phylogenetic evidence for the dispersal-vicariance interplay mediated by marine regression-transgression cycles. Journal of Biogeography 47(9): 1875–1887. https://doi.org/10.1111/jbi.13875

Dobat K (1975) Die Höhlenfauna der Schwäbischen Alb mit Einschluss des Dinkelberges, des Schwarzwaldes und des Wutachgebietes. Abhandlungen zur Karst- und Höhlenkunde, Reihe D, Paläontologie, Zoologie 2: 260–381.

Dobat K (1978) Die Höhlenfauna der Fränkischen Alb. Berichte der naturwissenschaftlichen Gesellschaft Bayreuth 16: 11–240.

Fišer C, Trontelj P, Luštrik R, Sket B (2009) Toward a unified taxonomy of *Niphargus* (Crustacea: Amphipoda): A review of morphological variability. Zootaxa 2061: 1–22. https://doi.org/10.11646/zootaxa.2061.1.1

Flot J-F, Wörheide G, Dattagupta S (2010) Unsuspected diversity of *Niphargus* amphipods in the chemoautotrophic cave ecosystem of Frasassi, central Italy. BMC Evolutionary Biology 10: e171. https://doi.org/10.1186/1471-2148-10-171

Foulquier A, Malard F, Lefébure T, Douady CJ, Gibert J (2008) The imprint of Quaternary glaciers on the present-day distribution of the obligate groundwater amphipod *Niphargus virei* (Niphargidae). Journal of Biogeography 35: 552–564. https://doi.org/10.1111/j.1365-2699.2007.01795.x

Fuchs A (2007) Erhebung und Beschreibung der Grundwasserfauna in Baden-Württemberg. PhD Thesis, university Koblenz-Landau, 109 pp.

Galassi DMP, Stoch F, Fiasca B, Di Lorenzo T, Gattone E (2009) Groundwater biodiversity patterns in the Lessinian Massif of northern Italy. Freshwater Biology 54: 830–847. https://doi.org/10.1111/j.1365-2427.2009.02203.x

Ginet R. (1996) Bilan systématique du genre *Niphargus* en France. Société Linneéenne de Lyon, France, 243 pp.

Glückert G (1987) Zur letzten Eiszeit im alpinen und nordeuropäischen Raum. Geographica Helvetica 2: 93–98. https://doi.org/10.5194/gh-42-93-1987

Grimm R (2015) Absenk- und Aufstauversuche zur Erkundung unzugänglicher zusammenhängender Karsthohlräume in der phreatischen Zone im Nahbereich einer Zugangsstelle. Mitteilungen des Verbandes der deutschen Höhlen- und Karstforscher 61(3+4): 93–100.

Grimm R (2020) Die Sedimente der Blätterteighöhle am Aachtopf, Baden-Württemberg (Kat.-Nr. 8119/029). Mitteilungen des Verbandes der deutschen Höhlen- und Karstforscher 66(1+2): 12–19.

Günzler E (1964) Über den Verlust der endogenen Tagesrhytmik bei dem Höhlenkrebs *Niphargus puteanus puteanus* (Koch). Biologisches Zentralblatt 83: 677–694.

Horton T, Lowry J, De Broyer C, Bellan-Santini D, Coleman CO, Corbari L, Costello, MJ, et al. (2021) World Amphipoda Database. World Register of Marine Species. http://www.marinespecies.org [Accessed 21 July 2021]

Jurado-Rivera JA, Álvarez G, Caro JA, Juan C, Pons J, Jaume D (2017) Molecular systematics of *Haploginglymus*, a genus of subterranean amphipods endemic to the Iberian Peninsula (Amphipoda: Niphargidae). Contributions to Zoology 86: 239–260. https://doi.org/10.1163/18759866-08603004

Kalyaanamoorthy S, Minh BQ, Wong TKF, von Haeseler A, Jermiin LS (2017) ModelFinder: fast model selection for accurate phylogenetic estimates. Nature Methods 14: 587–589. https://doi.org/10.1038/nmeth.4285

Karaman S (1932) 5. Beitrag zur Kenntnis der Süsswasser-Amphipoden. Prirodoslovne Razprave 2: 179–232.

Katoh K, Rozewicki J, Yamada KD (2019) MAFFT online service: multiple sequence alignment, interactive sequence choice and visualization. Briefings in Bioinformatics 20: 1160–1166. https://doi.org/10.1093/bib/bbx108

Lefébure T, Douady CJ, Gouy M, Gibert J (2006) Phylogeography of a subterranean amphipod reveals cryptic diversity and dynamic evolution in extreme environments. Molecular Ecology 15: 1797–1806. https://doi.org/10.1111/j.1365-294X.2006.02888.x

McInerney CE, Maurice L, Robertson AL, Knight RFD, Arnscheidt J, Venditti C, Dooley JSG, Mathers T, Matthijs S, Erikkson K, Proudlove GS, Hänfling B (2014) The Ancient Britons: Groundwater fauna survived extreme climate changes over tens of millions of years across NW Europe. Molecular Ecology 23: 1153–1166. https://doi.org/10.1111/mec.12664

Minh BQ, Schmidt HA, Chernomor O, Schrempf D, Woodhams MD, von Haeseler A, Lanfear R (2020) IQ-TREE 2: new models and efficient methods for phylogenetic inference in the genomic era. Molecular Biology and Evolution 37: 1530–1534. https://doi.org/10.1093/molbev/msaa015

Puillandre N, Lambert A, Brouillet S, Achaz G (2012) ABGD, Automatic Barcode Gap Discovery for primary species delimitation. Molecular Ecology 21: 1864–1877. https://doi.org/10.1111/j.1365-294X.2011.05239.x

Schellenberg A (1932) Deutsche subterrane Amphipoden. Zoologischer Anzeiger 99: 311–323.

Schellenberg A (1933a) Weitere deutsche und ausländische Niphargiden. Zoologischer Anzeiger 102: 22–33.

Schellenberg A (1933b) Die Niphargen des Brüsseler naturhistorischen Museums. Bulletin du Musée royal d'Histoire naturelle de Belgique 9: 1–8.

Schellenberg A (1936) Amphipodenstudien in Südbaden. Sitzungsberichte der Gesellschaft naturforschender Freunde Berlin 1936: 23–34.

Schetter H, Knupfer H, Grygoruk B (2017) Der Schwarze Brunnen. Das Portal in den Zollergraben, 113 pp.

Schwarz G (1978) Estimating the dimension of a model. The Annals of Statistics 6(2): 461–464. https://doi.org/10.1214/aos/1176344136

Spangenberg H (1973) Faunistisch-ökologische Untersuchungen an Gewässern von Gipshöhlen und in Grundwässern des Südharzes und des Kyffhäusers. Internationale Revue der gesamten Hydrobiologie 58: 501–542. https://doi.org/10.1002/iroh.19730580404

Spöri Y, Flot J-F (2020) HaplowebMaker and CoMa: two web tools to delimit species using haplowebs and conspecificity matrices. Methods in Ecology and Evolution 11(1): 1434–1438. https://doi.org/10.1111/2041-210X.13454

Straub R (2013) Die Wimsener Höhle: Expedition in die tiefste Unterwasserhöhle Deutschlands. Ostfildern, Thorbecke, 112 pp.

Verovnik R, Sket B, Trontelj P (2005) The colonization of Europe by the freshwater crustacean *Asellus aquaticus* (Crustacea: Isopoda) proceeded from ancient refugia and was directed by habitat connectivity. Molecular Ecology 14: 4355–4369. https://doi.org/10.1111/j.1365-294X.2005.02745.x

Weber D (1991) Die Evertebratenfauna der Höhlen und künstlichen Hohlräume des Katastergebietes Westfalen einschließlich der Quellen- und Grundwasserfauna. Abhandlungen zur Karst- und Höhlenkunde 25, 701 pp.

Weber D (2012) Die Höhlenfauna und -flora des Höhlenkatastergebietes Rheinland-Pfalz/Saarland, 5. Teil. Abhandlungen zur Karst- und Höhlenkunde 36, 2367 pp.

Weber D, Flot J-F, Weigand H, Weigand AM (2020a) Demographic history, range size and habitat preferences of the groundwater amphipod *Niphargus puteanus* (C.L. Koch in Panzer, 1836). Limnologica 82: 125765. https://doi.org/10.1016/j.limno.2020.125765

Weber D, Stoch F, Knight L, Chauveau CA, Flot J-F (2020b) The genus *Microniphargus* (Crustacea, Amphipoda): evidence for three lineages distributed across northwestern Europe and transfer to Pseudoniphargidae. bioRxiv 2020.08.25.266817v1. https://doi.org/10.1101/2020.08.25.266817

Weber D, Brad T, Stoch F, Flot J-F (2021) Supporting data for the article "Rediscovery and redescription of *Niphargus enslini* Karaman, 1932 (Amphipoda, Niphargidae) in southern Germany". Zenodo. https://doi.org/10.5281/zenodo.5413630

Zaenker S (2008) Das Biospeläologische Kataster von Hessen. Die Fauna der Höhlen, künstlichen Hohlräume und Quellen. Abhandlungen zur Karst- und Höhlenkunde 32, CD version.

Supplementary material 1

Tables S1–S4, Figure S1

Authors: Dieter Weber, Traian Brad, Fabio Stoch, Jean-François Flot

Data type: pdf. file

Explanation note: **Table S1**. List of primers used for amplification and sequencing and PCR amplification conditions. **Table S2**. Species (in alphabetical order) and Gen-Bank accession numbers of the 28S sequences (GB 28S) used in the phylogenetic analysis. Outgroup genera and species used in the analysis are reported in bold. **Table S3**. Species, voucher codes, sites, geographical coordinates (WGS84), collectors and date of collection and GenBank accession numbers of the COI sequences used in the haplotype network. **Table S4**. Morphometric data (length of body, head, telson and length and width of articles of appendages) of the male of *Niphargus enslini* collected in the Blätterteighöhle (measures in mm). **Figure S1**. Phylogenetic tree positioning *Niphargus enslini* within the wider phylogeny of the genus *Niphargus*, constructed using maximum likelihood (IQTree2), based on a fragment of the 28S rRNA gene. Ultrafast bootstrap supports are shown on nodes. The *N. virei* clade, which includes *N. enslini* (100% support), is reported in red. Four Pseudoniphargidae were used as outgroups.

Link: https://doi.org/10.3897/subtbiol.40.73017.suppl1